

Chapter 4

Gravitational lensing by global monopole

4.1 Introduction:

Some quantum field theories admit formation of topological defects of different kinds during phase transitions in the early universe as a consequence of spontaneous breaking of symmetry. The topological defects are classified depending on the topology of vacuum manifold. A monopole may form when manifold contains surfaces those cannot be continuously shrunk to a point. When monopole is formed through spontaneous breaking of a gauge symmetry the resultant configuration has finite energy and its mass is condensed in a very tiny core. The produced monopole configuration thereby behaves like an elementary particle. Instead if monopole is resulted from breakdown of a global symmetry, the produced configuration has linearly divergent mass owing to the long range Nambu-Goldstone field. The typical distance between global monopole and anti-monopoles will be of the horizon size if such global monopole formed in the early universe and that gives a natural cut-off of the energy density of global monopole system.

The gravitational field due to a global monopole can be quite strong because of large energy density associated with Nambu-Goldstone field surrounding the monopole. The exterior space time metric due to global monopole is asymptotically non flat due to the long range Nambu-Goldstone field with energy density decreasing with the distance as r^{-2} [149]. Interestingly such kind of variation

(as r^{-2}) of energy density of global monopole configuration has been exploited to explain the flatness of rotation curves of stars and gases at the outer part of several galaxies [150]. An important feature of the global monopole configuration is that for minimally coupled to gravity system the effective mass in the tiny core of the system is negative that leads to a repulsive potential. As a result no bound orbits exist for the global monopole configuration those are minimally coupled to gravity [149, 151]. Such lack of bound orbits feature can be avoided by considering some nonminimal couplings of global monopole configuration to gravity [152]. Alternatively if a global monopole is swallowed by a black hole at the centre of a galaxy, the resultant configuration admits bound orbit as the effective mass of the system becomes positive and it also can describe the observed flat rotation curve of galaxies.

Gravitational lensing studies provide important clue about mass distribution of the universe including the presence of dark matter [153, 154]. It is also an important tool to probe the nature of space-time geometry of gravitational lenses [153, 155]. The theory of lensing has been developed in stages by many authors including Einstein himself [156]. The deflection angle in weak field regime is usually evaluated exploiting post-parametrized Newtonian formalism that incorporate General Relativity and many other modified theories [153, 155]. The observational consequences of weak lensing were primarily suggested by Chwolson [158] and Zwicky [157]. The lensing theory in strong field regime of Schwarzschild space time was mainly developed by Virbhadra and Ellis [159] and Frittelli and Newman [160]. The lens equation without weak-field or small angle approximations was first introduced in [159, 161] and the observational features of the strong lensing phenomena was explored in [159] by treating the massive black hole of the galactic Centre as Schwarzschild lens. A few interesting works (not exhausted) considering other static spherical symmetric lens in strong field can be found in Refs. [162–164].

The light propagation in space time of a global monopole is well studied in the chapter both weak field [164–166] and strong field [167] regime. In [165] the deflection angle is obtained from the geodesic equations exploiting standard integration method. The strong gravitational lensing of a Schwarzschild black hole with a solid deficit angle owing to a global monopole is studied in [167] applying Bozza's analytical technique [168].

Conventionally the quantum of bending of light rays due to a lens (massive deflector) is derived from null geodesic equations in the neighborhood of the lens

describing it (the lens) by an appropriate space time metric. Recently Rindler and Ishak [54] have claimed that the conventional prescription does not yield complete result of deflection angle in general, particularly when the space-time metric is asymptotically non flat. Working with the Schwarzschild-de Sitter (SDS) geometry [130], they demonstrated that contrary to the conventional result there is a small contribution of cosmological constant Λ in the bending though the orbital equation for light in SDS space-time is free from Λ . In their prescription (for obtaining bending angle) the contribution of Λ to the bending angle comes from the space-time metric itself. Note that according to Rindler and Ishak [54] null geodesic equation and its integral are only the ‘half story’ in estimating the bending angle, the space-time metric itself constitutes the remaining part of the story.

While estimating gravitational bending due to global monopole the effect of asymptotically non-flat geometry of global monopole space-time is usually not considered in the chapter, which is precisely our objective of the present study. In this target we shall apply the Rindler-Ishak method for estimation of bending angle and thereby the influence of asymptotically non-flat geometry, if any, on gravitational lensing by global monopole space-time will be examined. Consequently we shall look for proper detectable signature of global monopole through gravitational lensing studies. We shall employ our findings to examine the consistency of global monopole hypothesis as an alternative to dark matter in galaxies.

The plan of the chapter is the following. In the next section(4.2) we would present the exterior Barriola-Vilenkin space-time due to a global monopole. In section 4.3 we briefly describe the technique to be adopted for estimation of bending angles. In section 4.4 we would estimate gravitational bending due to global monopole metric. In section 4.5 we shall investigate gravitational bending for space-time due to a Schwarzschild black hole that swallowed a global monopole. The image position and magnification of images in weak gravitational lensing due to a Schwarzschild black hole that swallowed a global monopole will be described in section 4.6. We shall discuss our findings in section 4.7 and we shall conclude in the same section.

4.2 The space-time metric due to global monopole

A simplest model that gives rise to a global monopole consists of a self-coupling scalar field triplet φ^a ($a = 1, 2, 3$ the internal $O(3)$ index) whose original global $O(3)$ symmetry is spontaneously broken to $U(1)$. The Lagrangian of the model is described by (we are working in units such that $G = c = \hbar = 1$)

$$L = \frac{1}{2} \partial_\mu \varphi^a \partial^\mu \varphi^a - \frac{\lambda}{4} (\varphi^a \varphi^a - \eta^2)^2 \quad (4.1)$$

where η represents the scale of symmetry breaking and λ is a constant of the model. The configuration describing a monopole is given by the ansatz

$$\varphi^a = \eta f(r) \frac{x^a}{r} \quad (4.2)$$

with $x^a x^a = r^2$. In flat space $f(r) = 1 - (\lambda \eta^2 r^2)^{-1}$. Hence outside the core of a global monopole $f(r) \approx 1$. Accordingly the energy momentum tensor can be approximated as $T_t^t \approx T_r^r \approx \eta^2/r^2$ and $T_\theta^\theta \approx T_\phi^\phi \approx 0$. Barriola and Vilenkin [149] derive the gravitational field for the configuration from the Einstein equations which is given by

$$ds^2 = - \left(1 - 8\pi\eta^2 - \frac{2M}{r} \right) dt^2 + \left(1 - 8\pi\eta^2 - \frac{2M}{r} \right)^{-1} dr^2 + r^2 (d\theta^2 + \sin^2 \theta d\phi^2) \quad (4.3)$$

with $M = M_{GM}$, $M_{GM} \sim -\frac{16\pi}{3} \lambda^{-1/2} \eta$ denotes the effective mass of the global monopole.

Interestingly for $M = 0$ (in equation (4.3)), the curvature tensor components are $R_0^0 = R_1^1 = R_{01} = 0$, $R_2^2 = \frac{1-8\pi\eta^2}{r^2}$ and hence the curvature of the space time remains non-zero.

Since the effective mass M is negative, the gravitational potential due to global monopole is repulsive. Consequently the space-time does not admit any bound orbit for test particles [149, 151]. For reasonable values of λ and η , M is very small

on the astrophysical scale. Thus neglecting the tiny negative mass at the core the global monopole metric reads as

$$ds^2 = - (1 - 8\pi\eta^2) dt^2 + (1 - 8\pi\eta^2)^{-1} dr^2 + r^2 (d\theta^2 + \sin^2 \theta d\phi^2) \quad (4.4)$$

that can be recast as

$$ds^2 = -dt^2 + dr^2 + (1 - 8\pi\eta^2) r^2 (d\theta^2 + \sin^2 \theta d\phi^2) \quad (4.5)$$

which describes a space with a deficit angle $\Delta = 8\pi\eta^2$; in this configuration the surface area of a sphere of radius r is $4\pi\Delta r^2$ instead of $4\pi r^2$.

If we restrict to the equatorial plan ($\theta = \pi/2$), the metric (4.5) reduces to $ds^2 = -dt^2 + dr^2 + (1 - \Delta) r^2 d\phi^2$ which becomes locally Minkowskian under a coordinate transformation $\phi' = \sqrt{1 - \Delta}\phi$. Thus light path should remain unperturbed by the presence of global monopole space time. The space time geometry around global monopole in equatorial plan, however, is not globally Minkowskian because ϕ' changes from 0 to $\sqrt{1 - \Delta}2\pi$. Therefore, light rays while propagating in the equatorial plan of the metric 4.4 would suffer a bending by $\sim \Delta\pi/2$.

The spherically symmetric gravitational collapse of the matter around a global monopole leads to formation of a black hole [165] (alternatively a black hole can swallow a global monopole) and thereby a black hole can possess 'hair' in the form of topological charge.

4.3 Methodology for estimation of bending angle

Before addressing the deflection of light rays in the case of asymptotically non-flat space-time let us first quickly review the basic approach of calculating bending of light due to gravity in asymptotically flat space-time.

The geometrical configuration for the phenomenon of gravitational bending of light is given in Figure (4.1). The light emitted by the distant source S is deviated by the

gravitational source (Lens) L and reaches the observer O. The angle of deflection (α) is the difference between the angle of emission (from the source) and the angle of reception (by the observer) minus π . The angles are to be measured with respect to a common polar axis which is usually taken as the line joining the observer and the center of the lens (OL), the so called optic axis or a line perpendicular to it that passes through the Centre of the lens. If both the observer and the source are situated in the flat space-time region and if tangents are drawn to the null geodesic at the source and image positions, which are represented by SQ and IO in Figure (4.1)(considering the space-time away from the lens is flat), and if C is their point of intersection (if there were no lensing object present) then $\angle OCJ$ will be the angle of deflection (α) by the lens.

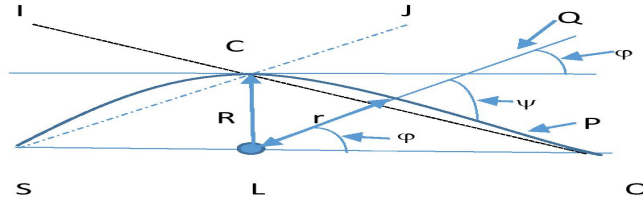


FIGURE 4.1: Lensing diagram - the source S emits light rays which reach the observer O after being gravitationally deflected by the lens L.

The null geodesic equation of light in flat space time is $\frac{d^2u}{d\phi^2} + u = 0$, where $u = 1/r$. Hence the orbit equation of undeflected (straight line) light ray in flat space not containing the pole (the centre of the lens in the lensing configuration) is given by $u = u_o \sin(\phi - \phi_o)$, where $r_o = 1/u_o$ is the perpendicular distance from the Centre of the lens to the path of the light rays and ϕ_o is the angle that the light rays made with the polar axis at the point of intersection. For simplicity of calculations the direction of the polar axis is normally taken either parallel or perpendicular to the undeflected light rays which corresponds to $\phi_o = 0$ or $-\pi/2$ respectively. In the

case of weak gravitational field one expects that the light path will be deviated by a small amount from the straight line path and one explores for a solution of the orbit on that (perturbation) basis [56].

For asymptotically flat space-time and when the source and observers are far away (in compare to the length scale of the impact parameter which is the perpendicular distance from the center of the lens to the tangent to the null geodesic at the source) from the lens, the direction of light orbit at source position (observer) may be taken as the same to the direction of asymptotic light rays in the source (observer) region. Exploiting this feature one conventionally estimates the emission (reception) angle from the null geodesic equation by letting the radial distance to be infinitely large.

For asymptotically non-flat space time letting $r \rightarrow \infty$ to obtain the asymptotes of the orbit is not proper. This is because the direction of light rays at the source (observer) position may not be the same to the direction of asymptotic light rays. For instance, in the case of Schwarzschild-de Sitter space time the direction of light rays at the source (observer) position will not be the same to that at any other (distant) points owing to the non-flat character of the asymptotic space time. Hence the conventional approach is not strictly applicable for estimating bending angle in such a situation.

Rindler and Ishak prescribe a method for obtaining bending angle in asymptotically non-flat space time [54]. Their method is based on the invariant formula for the cosine of the angle between two coordinate directions P and Q

$$\cos(\psi) = \frac{g_{ij}P^iQ^j}{(g_{ij}P^iP^j)^{1/2}(g_{ij}Q^iQ^j)^{1/2}} \quad (4.6)$$

If P is taken as the direction of the orbit and Q is taken as that of the coordinate line $\phi = \text{constant}$ (Figure (4.1)), then one may write $P \equiv (dr, d\phi) = (dr/d\phi, 1)d\phi$, ($d\phi < 0$) and $Q \equiv (dr, 0) = (1, 0)dr$. Consequently for the general spherically symmetric space time metric $ds^2 = -f(r)dt^2 + f(r)^{-1}dr^2 + r^2(d\theta^2 + \sin^2\theta d\phi^2)$ the angle between P and Q directions becomes [55]

$$\tan(\psi) = \frac{rf(r)^{1/2}}{|dr/d\phi|} \quad (4.7)$$

The one-sided bending angle is then given by $\epsilon = \psi - \phi$.

4.4 Gravitational deflection of light due to global monopole

First we follow the conventional approach of calculating the bending angle. In the equatorial plane ($\theta = \pi/2$) the orbital equation for photon in monopole space-time (4.4) as obtained from the null geodesic equations is

$$\frac{d^2 u}{d\phi^2} + (1 - \Delta)u = 0 \quad (4.8)$$

where $u = 1/r$. The exact solution of the above equation reads

$$u = u_o \sin [(1 - \Delta)^{1/2} \phi] \quad (4.9)$$

where u_o is a constant, related to the closest distance parameter (r_o) through the relation $u_o = 1/r_o$. The asymptotes of the orbit can be obtained letting $r \rightarrow \infty$ which gives $\phi_\infty^1 = 0$ and $\phi_\infty^2 = \pi(1 - \Delta)^{-1/2}$. Hence the total bending (angle between the two asymptotes) is given by

$$\delta\phi = [(1 - \Delta)^{-1/2} - 1] \pi \quad (4.10)$$

For small Δ , the deflection angle becomes $\Delta\pi/2$, which was expected in view of the other form of the monopole metric (4.5).

Because of the asymptotically non-flat nature of global monopole space time we will now follow the prescription of Rindler and Ishak [54].

For the metric given by equation (4.4) we get from equation (4.9)

$$\frac{dr}{d\phi} = -u_o r^2 (1 - \Delta)^{1/2} \cos [(1 - \Delta)^{1/2} \phi] \quad (4.11)$$

Let us consider the situation that the source, lens and observer are perfectly aligned. So first we take $\phi = 0$ (corresponding to the source) as prescribed by Rindler and Ishak [54]. The equation (4.9) immediately implies $r \rightarrow \infty$ which means that the source has to be at infinity for an admissible photon trajectory

from the source with non-zero distance of closest approach. Because of asymptotically non-flat behavior of the space time geometry we don't prefer the choice of source at infinity. Let for the time being we consider that the source is at infinity. Consequently $\psi_o = 0$ as follows from the equation (4.7). Next consider $\phi = \pi$ for the observer which leads to $r = R/\sin[(1 - \Delta)^{1/2}\pi]$ where $R = 1/u_o$. The equation (4.7) then gives $\psi_\pi = (1 - \Delta)^{1/2}\pi$. Thus the total bending angle is

$$\begin{aligned}\delta\epsilon &= \psi_o - \phi_o + \psi_\pi - \phi_\pi \\ &= [(1 - \Delta)^{1/2} - 1] \pi \\ &\simeq -\Delta\pi/2\end{aligned}\tag{4.12}$$

which clearly differs from what we obtained in equation (4.10) using the conventional method. More importantly the deflection angle is negative. For small Δ the difference of deflection angle between two approaches becomes $\Delta\pi$. The difference in bending angle in two approaches appears to be due to asymptotic non-flat characteristics of the space time. The observer position differs in the two cases; in the conventional case the source and observers (asymptotes) are placed at $(r = \infty, \phi = 0)$ and $(r = \infty, \phi = \pi(1 - \Delta)^{-1/2})$ (otherwise the observer cannot see the deflected ray) respectively whereas the points $(r = \infty, \phi = 0)$ and $(r = R/\sin((1 - \Delta)^{1/2}\pi), \phi = \pi)$ are chosen in the Rindler-Ishak approach as coordinates of the source and observer. The tangent to the light orbit at the observer point, which is at finite distance away from the lens, makes a finite angle that leads the difference in the two estimates. Since the position of source and observer are pre-fixed in any real observations, it is rational to apply Rindler-Ishak method over the conventional method for estimation of deflection angle.

Now we shall estimate the bending angle also considering general position of source (ϕ_s, d_s) and observer (ϕ_o, d_o) [55, 169] without demanding a perfect alignment of the source, lens and observer. In such a case, we get from equation (4.7) through equations (4.9) and (4.11)

$$\begin{aligned}
\delta\epsilon_k &= \psi_k - \phi_k \\
&= [(1 - \Delta)^{1/2} - 1] \phi_k \\
&\simeq -\Delta\phi_k/2
\end{aligned} \tag{4.13}$$

where k stands for s and o (denoting respectively source and observer), so that the total deflection angle becomes

$$\begin{aligned}
\delta\epsilon &= \epsilon_s + \epsilon_o \\
&= [(1 - \Delta)^{1/2} - 1] (\phi_s + \phi_o) \\
&\simeq -\Delta/2 (\phi_s + \phi_o)
\end{aligned} \tag{4.14}$$

The expression for equation (4.12) can be retrieved from the above equation by putting $\phi_s = 0$ and $\phi_o = \pi$.

In view of the negative bending angle the lensing diagram for an isolated global monopole essentially looks like that given in the figure (4.2) below:

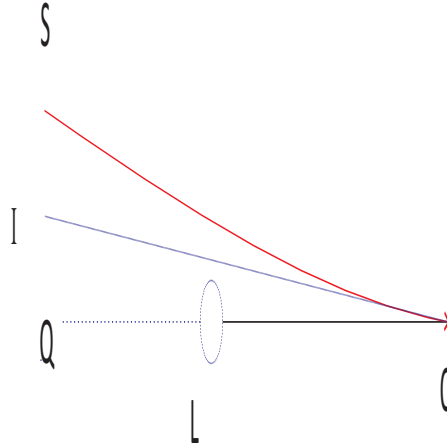


FIGURE 4.2: Lensing diagram - the source S emits light rays which reach the observer O after being gravitationally deflected by the lens L which is an isolated global monopole. The image position is denoted as I.

4.5 Bending of light due to a Schwarzschild black hole that swallowed a global monopole

The space time described by the global monopole metric does not have any event horizon around the monopole. It also does not admit any bound orbit [149, 151]. However, there will be an event horizon if a Schwarzschild black hole of mass greater than the effective (negative) mass of a global monopole swallows the monopole. This configuration also allows bound orbits. The metric that represents the configuration is that given by equation (4.3) with $M = M_{bh} - M_{GM}$ is the difference of the mass (M_{bh}) of the Schwarzschild black hole and the effective (negative) mass (M_{GM}) of the monopole. We will now consider bending of light exploiting both the conventional and the Rindler-Ishak methods [54].

Proceeding exactly the same way as in the preceding section the orbital equation for photon in this case is given by

$$\frac{d^2u}{d\phi^2} + (1 - \Delta)u = 3Mu^2 \quad (4.15)$$

Adopting usual perturbation approach, the solution of the above equation to the first order in M reads

$$u = u_o \sin [(1 - \Delta)^{1/2} \phi] + \frac{3Mu_o^2}{2(1 - \Delta)} \left(1 + \frac{1}{3} \cos [2(1 - \Delta)^{1/2} \phi] \right) \quad (4.16)$$

At the distance of closest approach r_o , $dr/d\phi$ vanishes which gives the relation

$$\frac{1}{r_o} = \frac{1}{R} \left(1 + \frac{M}{R(1 - \Delta)} \right) \quad (4.17)$$

For the asymptotes of the orbit we let $r \rightarrow \infty$ and consequently the above equation gives $\phi_\infty^1 \approx -\frac{2M}{R}(1 - \Delta)^{-3/2}$ and $\phi_\infty^2 \approx \pi(1 - \Delta)^{-1/2} - \frac{2M}{R}(1 - \Delta)^{-3/2}$. Hence the total bending in the first of $\frac{M}{R}$ is given by

$$\begin{aligned}
\delta\phi &= [(1 - \Delta)^{-1/2} - 1] \pi + \frac{4M}{R}(1 - \Delta)^{-3/2} \\
&\simeq \Delta\pi/2 + \frac{4M}{R(1 - \Delta)^{3/2}} \\
&\simeq \Delta\pi/2 + \frac{4M}{R} + \frac{6\Delta M}{R}
\end{aligned} \tag{4.18}$$

which is what obtained in [165]. Now we will estimate the bending following the prescription of Rindler and Ishak i.e. vide equation (4.7). Differentiating equation (4.16) we get

$$\begin{aligned}
\frac{dr}{d\phi} &= -u_o r^2 (1 - \Delta)^{1/2} \cos(1 - \Delta)^{1/2} \phi - \\
&\quad Mr^2 u_o^2 (1 - \Delta)^{-1/2} \sin [2(1 - \Delta)^{1/2} \phi]
\end{aligned} \tag{4.19}$$

When $\phi = 0$, the equation (4.16) suggests that it occurs when $r = \frac{R^2}{2M}(1 - \Delta)$. Consequently the equation (4.7) gives that to the first order in M , $\psi_o = \frac{2M}{R(1 - \Delta)}$. On the other hand when $\phi = \pi$, $1/r \approx \frac{1}{R} \sin((1 - \Delta)^{1/2} \pi) + \frac{2M}{R^2(1 - \Delta)}$. When Δ is small, the equation (4.7) gives $\psi_{pi} = \pi - \Delta\pi/2 + \frac{2M}{R(1 - \Delta)}$. Thus the total bending angle is

$$\delta\epsilon = \psi_o + \psi_\pi - \pi = -\Delta\pi/2 + \frac{4M}{R(1 - \Delta)} \tag{4.20}$$

One can recover the usual bending expression for the Schwarzschild space time from the above equation for $\Delta = 0$. Again it has been noted that the above expression of bending is not equal to that obtained by the conventional approach as given by equation (4.18).

4.6 Image position and magnification in weak lensing by global monopole space time

The angular position of the images (ζ) can be obtained from the lens equation as given below [159]

$$\tan \zeta - \tan \beta = \frac{d_{ls}}{d_{os}} [\tan \zeta + \tan(\delta\epsilon - \zeta)] \quad (4.21)$$

where β denotes the angular source position, α is the deflection angle, d_{ls} and d_{os} are the distances between lens and source and observer and source respectively. For positive β , the above relation only gives images on the same side ($\zeta > 0$) of the source. Images on the other side can be obtained by taking negative values of β .

When the source, lens and observer are aligned i.e. when β is small, the lens equation in the weak lensing scenario ($\delta\epsilon$ small) reduces to

$$\beta = \zeta - \frac{d_{ls}}{d_{os}} \delta\epsilon \quad (4.22)$$

The image positions can be obtained from the above equation after inserting the expression for bending angle from equation (4.20) which leads to

$$\zeta_{\pm} = \frac{1}{2} \left(\beta' \pm \sqrt{4\alpha'_0 + \beta'^2} \right) \quad (4.23)$$

where the indices \pm denote the parities of the images, where

$$\beta' = \beta - \frac{d_{ls}}{d_{os}} \Delta \frac{\pi}{2}, \quad (4.24)$$

and

$$\alpha'_0 \equiv \sqrt{\frac{d_{ls}}{d_{ol}d_{os}} \frac{4M}{1 - \Delta}}. \quad (4.25)$$

The form of the equation (4.23) is exactly same to the expression of image position in lensing by Schwarzschild black hole. When $\Delta = 0$, the equation (4.23) reduces to the expression of the image positions due to Schwarzschild lens. It appears that the role of the second term in the right side of equation (4.24) is just of an off-set angle. A point to be noted that for formation of Einstein-Chwolson ring in the present case the source has to be at $\beta = \frac{d_{ls}}{d_{os}} \Delta \frac{\pi}{2}$ instead of $\beta = 0$.

The magnification of the image (the ratio of the flux of the image to the flux of the unlensed source) when the lens is a Schwarzschild black hole that swallowed a global monopole is given by

$$\begin{aligned}\mu_{\pm} &= \frac{1}{(\beta/\zeta_{\pm})\partial\beta/\partial\zeta_{\pm}} \\ &= \frac{1}{4} \left[\frac{\beta'}{\sqrt{\beta'^2 + 4\alpha_0'^2}} + \frac{\sqrt{\beta'^2 + 4\alpha_0'^2}}{\beta'} \pm 2 \right]\end{aligned}\quad (4.26)$$

The form of the above expression is again the same to that of Schwarzschild lensing case. In figure (4.3) the image magnifications are shown as a function of normalized source position in gravitational lensing by a Schwarzschild black hole that swallowed a global monopole considering $\frac{d_{ls}}{d_{os}} = 0.9$. The results are compared with magnification in lensing by a Schwarzschild black hole.

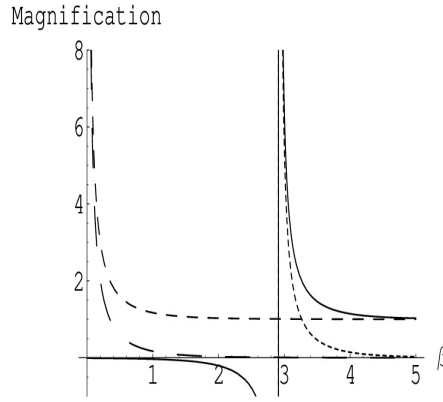


FIGURE 4.3: Magnification in weak gravitational lensing - the solid line and dotted line respectively denote μ_+ and μ_- due to lensing by a Schwarzschild black hole that swallowed a global monopole, the dashed line and long dashed line respectively denote μ_+ and μ_- due to lensing by a Schwarzschild black hole.

The ratio of magnifications of two images is given by

$$\frac{\mu_+}{\mu_-} = \left[\frac{\sqrt{\beta'^2 + 4\alpha_0'^2} + \beta'}{\sqrt{\beta'^2 + 4\alpha_0'^2} - \beta'} \right]^2 \quad (4.27)$$

4.7 Discussion & Conclusion

We have estimated gravitational deflection angle due to a global monopole and a Schwarzschild black hole that swallowed a global monopole using Rindler-Ishak prescription. The signatures of gravitational bending due to global monopoles

as obtained from the present analysis include i) the deflection angle is negative, ii) the magnitude of the angle is nearly constant iii) it is independent of impact parameter.

Clearly for the stated space time geometries the quantum of bending angles obtained with Rindler-Ishak method differ significantly from those obtained with conventional technique owing to asymptotic non-flat characteristics of the stated space times. The Rindler-Ishak method appears to be more flexible; it reproduces the results obtained in conventional approach when source and observer are placed at large distances when the space time metrics are asymptotically flat. However, when source and/or observer are at finite distance away from the lens or if the space time is not flat asymptotically, Rindler-Ishak technique offers a way to estimate the true bending angle and consequently to obtain the image positions.

Global monopole or rather a Schwarzschild black hole that swallowed a global monopole at the center of a galaxy has been proposed in the chapter as an alternative to dark matter hypothesis owing to inverse square of distance variation of the energy density of the global monopole configuration that correctly describe the observed flat rotation curve of galaxies. Interestingly for a symmetry breaking scale of $\eta \sim 10^{16}$ GeV the equivalent Newtonian mass contained within typical galactic radius of $r_{gal} \sim 15$ kpc turns out to be $\Delta r_{gal} \sim 10^{69}$ GeV which is an order higher than the luminous mass of the galaxy [150]. The presence of dark matter is already indicated by several gravitational lensing measurements; several lensing observations such as the Sloan Digital Sky Survey [170], the Hubble Space Telescope [171] missions indicate the presence of an order larger extra mass over the luminous mass of the lensing object particularly when galaxy clusters are considered as lenses. The dark matter candidature of global monopole system is not consistent with such lensing observations as is explained below citing the case of Abell 370 cluster.

The ‘giant luminous arcs’ were first observed in rich galaxy cluster Abell 370 [172, 173] at redshift 0.374. The details analysis of the observed luminous arcs suggested that they were gravitationally lensed images of background galaxies [174–178]. Here our objective is to estimate the mass of the lensing galaxy Abell 370 from a giant luminous arc using equation (4.23) and compare the estimated mass with the luminous mass obtained independently from photometric study

TABLE 4.1: Estimated mass of Abell 370

Object	z_l	z_s	r_E in arcsecs	$M/M_\odot \times 10^{-11}$ Global monopole	$M/M_\odot \times 10^{-11}$ Schwarzschild
<i>Abell370</i>	0.374	0.724	25	923.06	923.07

[172, 173]. Generally galaxy clusters have complex matter distributions and cannot be considered to be either point masses or spherically symmetric but a spherically symmetric lens model can be employed as a first approximation to extract the same order of magnitude results as the more realistic case analyzing the large arcs that are observed in clusters [177, 178]. We have considered the longest arc, A0, which has a radius of curvature of about $25''$ [174] and treat it as an Einstein ring. The observed redshift (z_s) of A0 is 0.724 which gives the distance of the background galaxy. A concordance cosmological model of $(\Omega_m, \Omega_\Lambda, \Omega_k) = (0.3; 0.7; 0)$ is applied for distance estimation from redshifts of lens and source. Our findings are given in Table (4.1).

It is found that estimated mass of Abell 370 from the above stated simplified model is consistent, of the same order of magnitude, with Subaru weak-lensing measurements [179] and Hubble Space Telescope (HST) observations [180]. The estimated mass by treating the lens Abell 370 as a Schwarzschild space time that swallowed a global monopole does not differ significantly from that obtained by modeling the lens as pure a Schwarzschild space time. But when the global monopole system is considered as an alternative to dark matter, the estimated total mass of the lens Abell 370 will represent the mass of only the luminous matter in the cluster. This is in contrast to the GR case (pure Schwarzschild geometry) where the estimated total mass of Abell 370 is the sum of the luminous and presumed dark matter. The photometric measurement suggests that mass of the luminous matter in Abell 370 is at least two orders smaller than the total mass of Abell 370 [174]. Thus the lensing observations of Abell 370 does not support the alternative dark matter hypothesis of global monopole system.

It is worthwhile to mention that for lensing galaxy system of smaller luminous mass the contribution of global monopole (Δ) can be significant as may be seen from the figure (4.4) below where the variation of deflection angle with luminous mass

is shown for both pure Schwarzschild geometry and global monopole swallowed Schwarzschild geometry taking the closest distance parameter 100 kpc.

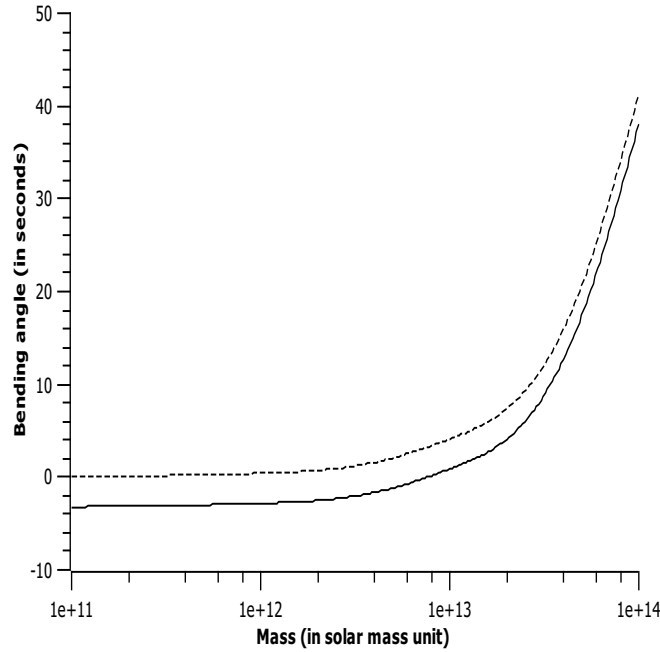


FIGURE 4.4: Variation of deflection angle with mass due to a pure Schwarzschild model (dotted line) and a global monopole swallowed Schwarzschild model (solid line). The closest distance parameter is taken 100 kpc.

The global monopole is an interesting class of topological defects and to look for possible observable effects of global monopole is important irrespective of its success/failure as an alternative to dark matter. In this chapter we have investigated about gravitational lensing signature of global monopole space time and improve the prevailing theoretical formulation of gravitational lensing by global monopole space time. The present findings should be useful in the search for global monopole through gravitational lensing observations.